

On The Shortest Collision-Free Path Planning for Manipulator Based on Circular Obstacle Region

An Kai*

Shandong Aerospace Electro-technology Institute, Shandong Yantai, 264670, China

Abstract: A model of collision-free path planning for manipulator's end-effectors based on circular obstacle regions and its corresponding algorithm to search the shortest collision-free path are presented in this paper. As the shortest one, the shortest collision-free path can be found from all the relative shortest collision-free paths whose definition and properties are provided as well in this paper. In order to find the relative shortest collision-free path, some algorithms on finding the common tangent of two circles and checking whether it lies on a certain relative shortest collision-free path are given. The searching algorithm of the shortest collision-free path is formed by integration of the algorithms. The searching algorithm does not contain any iterative procedure, and consequently it can effectively establish shortest collision-free paths for an acceptable short time. The searching algorithm can also avoid the trap of local minimum, and obtain the shortest collision-free path represented by a smooth and continuous curve connecting starting point and target point of the manipulator's end-effectors. In order to deal with the collision-free path planning based on non-circular obstacle regions, the concept of *expanded circle* is introduced, and the above-mentioned collision-free path planning method based on circular obstacle regions is generalized to non-circular obstacle regions. To resolve the intersection problem of the expanded circles, a method to surround an obstacle region by multi-circles and their common tangent segments is given in this paper.

Keywords: Manipulator, collision-free, path planning, circular obstacle region.

INTRODUCTION

Mobile robots are of great importance to applications that involve inhospitable or remote environments, inaccessible or dangerous to humans. Typical examples can be found in manufacturing, space exploration, security, medical surgery and the assistance of movement for the elder and handicapped people etc [1]. Although robots exist that use legs for locomotion, the most common terrestrial and space exploration robot platforms are wheeled. Tasks that go beyond inspection require a manipulator on-board.

Considering that a manipulator has to accomplish tasks by moving its end-effectors in the environment with ineluctable obstacles [2-4], it is essential for a manipulator to plan a collision-free path automatically.

The collision-free path planning problem is an optimization problem with the objective of computing an appropriate path between two specific locations. A feasible path is a path which does not collide with obstacles in the environment, regardless of different existing constraints that can be applied.

There are many ways to solve the obstacle avoidance problem of a manipulator, the most commonly used are the grid-based A* algorithm [5, 6], road maps [7], cell decomposition [8, 9] and artificial

potential field [10]. However, these methods are not perfect that every method has its own advantages and inevitable shortcomings. Artificial potential field method was proposed in 1986 by Dr. Khatib, and this method is first used in collision-free path planning for manipulators, and realized the real time obstacle avoidance. The main idea of artificial potential field method is establish attractive force potential field around target point and establish repulsive potential field around obstacles. The two potential fields together formed a new potential field, called artificial potential field. It searches for the falling direction of potential function to find a collision-free path which is built from the start point to target point. Because it is simple and intuitionistic, and uses little computation and small data storage space for planning collision-free paths and the path is smooth and secure. So the artificial potential field has been widely used. Then the artificial potential field method is a local planning method, which is difficult to plan the global optimal path. Algorithm itself also couldn't solve all local minimum problems. When the obstacle is very close to the target point or the robot on the straight line between target point and the obstacles, the robot will oscillate in front of the obstacle or be pushed by repulsion.

Grid method is more widely used in path planning. It divides environment space into several simple areas, called grids. Each cell is marked as an obstacle or a non-obstacle one based on the actual position of the obstacles. By such representation, the path can be defined as a consecutive sequence of grids which

*Address correspondence to this author at the Shandong Aerospace Electro-technology Institute, Shandong Yantai, 264670, China; E-mail: ankai2007@163.com

begins at the start grid and ends at the destination grid. In this way, there are many different algorithms developed such as: graph search methods [11], A* algorithm, ant colony [12] and genetic algorithm [13, 14] are some of these approaches. Grid method can provide the shortest collision-free path from the original starting point to the original target, but it cannot automatically give the smoothest path. Moreover, the shortest collision-free path provided by the method depends on the size of the grids, different sizes of the grids will cause different shortest collision-free path. On the other hand, the corresponding path searching algorithms, such as ant colony and genetic algorithm, require an iterative procedure, which can be time-consuming, and therefore it is difficult to guarantee the searching speed and precision. Especially these searching algorithms lack hill-climbing [15-17] capacity, and can easily fall in a trap of local minimum.

In computational geometry, the obstacles are modeled as polygons with disjoint interiors [18], which means that it is impossible for the shortest collision-free path to be a smooth curve. In this paper, a model of collision-free path planning for manipulator's end-effectors based on circular obstacle region and the corresponding algorithm to search the shortest collision-free path are presented in detail. The searching algorithm does not contain any iterative procedure, can avoid the trap of local minimum, and obtains the shortest collision-free path represented by a smooth and continuous curve connecting starting point and target point of the manipulator's end-effectors.

1. THE GEOMETRIC MODEL OF COLLISION-FREE PATH

In this section we introduce some of the basic notions and techniques used in collision-free path planning. The general collision-free path planning problem is quite difficult, and we shall make some simple assumptions.

The most drastic simplification is that we will look at a 2-dimensional collision-free path planning problem. The environment will be a planar region with circular obstacles. We assume that the radius of circles is large enough such that the manipulator's end-effectors can move along the circles without colliding with any of the obstacles. Considering that the presence of some circles region has no influence on the shortest collision-free path, we also assume that the projection of the center of each circle on the straight line connecting

starting point and target point always lies between the two points.

As shown in Figure 1, we denote the obstacles by disjoint circles with centers O_1, \dots, O_n and radii r_1, \dots, r_n respectively, and we denote starting point and end point of the manipulator's end-effectors by p_s and p_e .

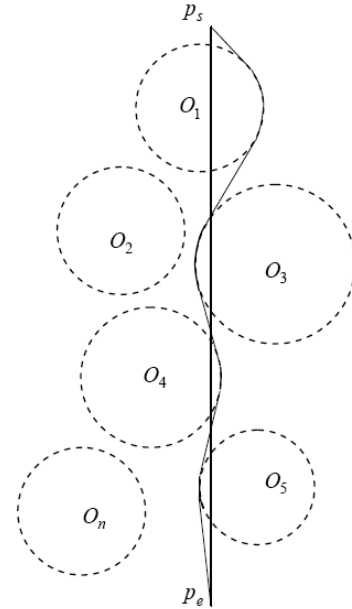


Figure 1: An obstacle avoidance path model of manipulator based on circular obstacle regions.

For two fixed points p_s and p_e , there are many collision-free path connecting them, which lie outside the obstacle regions, the projection of the obstacle on the planning plane. Therefore a collision-free path can partition the n disjoint circles into two groups, called a partition of the n disjoint circles generated by the collision-free path. Conversely, for each partition of the n disjoint circles, there are infinite collision-free path which can generate such a partition, one of them is the shortest collision-free path with respect to the partition, called relative shortest collision-free path with respect to the partition, or relative shortest collision-free path simply when no confusion is possible. Apparently the shortest collision-free path is the shortest one of all the relative shortest collision-free paths.

For any partition of the n disjoint circles, we will study the properties of relative shortest path. We can visualize what the relative shortest path looks like by a thought experiment. Imagine that the n disjoint circles are columns sticking out of the plane, take an elastic rubber band whose two endpoints are fixed at points p_s and p_e respectively, hold it around the columns, and let it go. It will snap around the columns, minimizing its length. The path shown by the elastic rubber band is the relative shortest collision-free path with respect to the partition. This discloses an

important property of a relative shortest collision-free path: it is a curve formed by the straight line segments and arc segments being connected alternately, whose first and last segments are all straight line segment. In particular, if the straight line segment $p_s p_e$ does not intersect each of the n circles, then the straight line segment $p_s p_e$ is the shortest collision-free path.

In this paper, the direction of a path or its sub-path connecting two points on the path is defined as the one from starting point and end point.

2. SOME PROPERTIES OF RELATIVE SHORTEST COLLISION-FREE PATH

In order to find a relative shortest collision-free path, it is useful to be aware of some properties of the relative shortest collision-free path. These properties include:

Property 2.1. For any relative shortest collision-free path, the straight line segment is tangent to the arc segment at their join point.

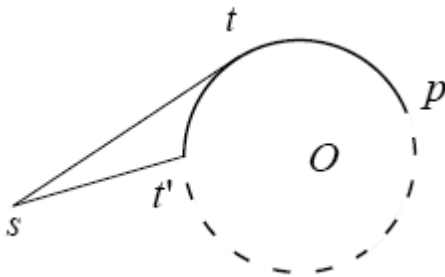


Figure 2: Connection of straight line and arc.

Proof: Actually, as shown in Figure 2, suppose for a contradiction that path $st'p$ is a sub-path of a relative shortest collision-free path L , and straight line segment st' is not tangent to arc segment $t'p$ at their join point t' . Then there is another straight line segment st that is tangent to the arc segment $t'p$ at their join point t . Since the total number of circles is finite, if point s is close to the circle adequately, straight line segment st will not intersect the other circles, and yet path stp is shorter than $st'p$. This contradicts the optimality of L , since any shortest path must be locally shortest, that is, any sub-path connecting points s and p on the path must be the shortest path from s to p .

However, property 1 gives only a necessary condition for a path to be a relative shortest collision-free path. Actually, as shown in Figure 3, for the sub-path $t_1 t_2 p t_3 t_4$, straight line segment $t_1 t_2$ is tangent to arc segment $t_3 p t_3$ at their join point t_2 , and straight line

segment $t_3 t_4$ is tangent to arc segment $t_3 p t_3$ at their join point t_3 . But directed straight line segment $t_1 t_2$ points to the counterclockwise direction of circle O , and directed straight line segment $t_3 t_4$ points to the clockwise direction of circle O . Before state other properties, we give the following definition firstly:

2.1. Definition

As shown in Figure 3, two directed tangent segments of the circle (or arc) O are called *consistent* with respect to circle(or arc) O , if they point to the same direction of circle(or arc) O .

By definition 2.1, two directed tangent segments of the arc $t_2 t_3$, or directed straight line segments $t_1 t_2$ and $t_3 t_4$ are not consistent with respect arc $t_2 t_3$. So we have:

Property 2.2. For any relative shortest collision-free path, if two straight line segments are tangent to an arc segment C at their join point, then the two straight line segments are consistent with respect the arc segment C .

Proof: As shown in Figure 3, suppose for a contradiction that path $t_1 t_2 p t_3 t_4$ is a sub-path of a relative shortest collision-free path L , p' is a point in straight line segment $t_3 t_4$. Since the total number of circles is finite, if two points p and p' are close to point t_3 adequately, straight line segment pp' will not intersect the other circles, and the path $t_1 t_2 pp' t_4$ will be shorter than path $t_1 t_2 p t_3 t_4$. This contradicts the optimality of L , since any shortest path must be locally shortest, that is, any sub-path connecting points t_1 and t_4 on the path must be the shortest path from t_1 to t_4 .

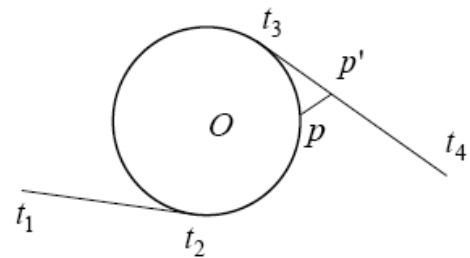


Figure 3: Connection of the arc and its two tangents (1).

If two straight line segments are tangent to an arc segment C at their join point, in order to test whether they are consistent, we first have to know whether the two straight line segments point to the same direction of arc C .

Then the direction vector of the directed straight line segment $t_1 t_2$ can be expressed as;

$$\vec{s}_1 t_1 = (x(t_2) - x(t_1), y(t_2) - y(t_1))$$

The radius vector at point t_2 can be expressed as

$$\vec{O}t_2 = (x(t_2) - x(O), y(t_2) - y(O))$$

So we have

$$\begin{vmatrix} x(t_2) - x(O) & y(t_2) - y(O) \\ x(t_2) - x(t_1) & y(t_2) - y(t_1) \end{vmatrix} > 0 \quad (1)$$

But for the directed straight line segment $t_3 t_4$, its direction vector can be expressed as

$$\vec{t}_3 t_4 = (x(t_4) - x(t_3), y(t_4) - y(t_3))$$

The radius vector at point t_3 can be expressed as

$$\vec{O}t_3 = (x(t_3) - x(O), y(t_3) - y(O))$$

So we have

$$\begin{vmatrix} x(t_3) - x(O) & y(t_3) - y(O) \\ x(t_4) - x(t_3) & y(t_4) - y(t_3) \end{vmatrix} < 0 \quad (2)$$

In fact, inequality (1) means that directed straight line segment $t_1 t_2$ points to the counterclockwise direction of circle O , but inequality (2) means that directed straight line segment $t_3 t_4$ points to the clockwise direction of circle O . Using the above determinant-based inequalities we can conclude that the two directed straight line segments point to the different direction of circle O .

Property 2.3. For any relative shortest collision-free path, each of its arc segments must be an inferior arc.

Proof: As shown in Figure 4, the arc $t_2 p' t_3$ is a superior arc, and the arc $t_2 p t_3$ is an inferior arc. It is impossible for the path $t_1 t_2 p' t_3 t_4$ to be a sub-path of a relative shortest collision-free path L , since path $t_1 t_2 p t_3 t_4$ is a shorter path from t_1 to t_4 .

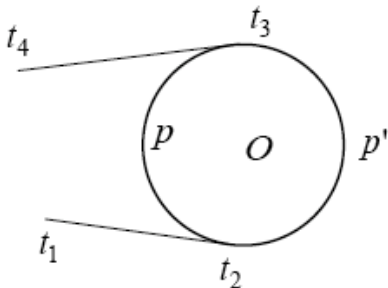


Figure 4: Connection of the arc and its two tangents (2).

Apparently, path $t_1 t_2 p' t_3 t_4$ is not a sub-path of any relative shortest collision-free path according to the proof of property 2.2.

Property 2.4. A relative shortest collision-free path intersects each of the circles at most once.

Proof: Suppose for a contradiction that a relative shortest collision-free path L intersects the circle O twice. As shown in Figure 5, suppose the path intersects the circle O in arc $t_2 t_3$ for the first time, since it can not contain any ring, it has to intersect the rest part of the circle O at a point p , for example. The dashed in Figure 5 denotes an arbitrary sub-path from t_4 to p . However the path $t_1 t_2 t_3 p$ is shorter than path $t_1 t_2 t_3 t_4 p$. This contradicts the definition of optimality of L .

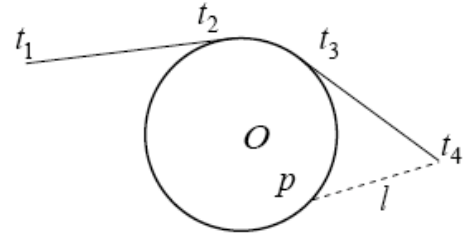


Figure 5: A path intersecting the circle twice.

3. SOME ALGORITHM ON FINDING THE COMMON TANGENT

From property 2.1 we know that in a relative shortest collision-free path, the straight line segment is tangent to arc segment at their join point, thereby two arc segments have to be connected by their common tangent. Finding all the common tangents in a relative shortest collision-free path is equivalent to finding relative shortest collision-free path. Therefore some algorithm on finding the common tangent of circles will be given in this section.

3.1. Circle's tangents passing through a point outside the circle

As shown in Figure 6, $p(x, y)$ is a point outside of the circle with center O_1 and radii r_1 , pp' is a tangent of circle O_1 passing through $p(x, y)$, it makes θ degree angles with the positive x-axis. Then the coordinates of tangent point p' can be expressed as $(r_1 \cos \theta, r_1 \sin \theta)$. For the purpose of finding the tangents passing through $p(x, y)$, it is sufficient to find the two tangent segments.

Since the vector $(r_1 \cos \theta, r_1 \sin \theta)$ is perpendicular to the vector

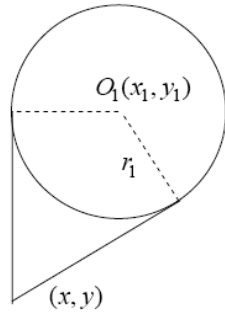


Figure 6: Tangents passing through a point in outside of the circle.

$$(r_1 \cos \theta, r_1 \sin \theta) + (x_1 - x, y_1 - y)$$

we have

$$r_1 \cos \theta (r_1 \cos \theta + x_1 - x) + r_1 \sin \theta (r_1 \sin \theta + y_1 - y) = 0$$

$$r_1 + (x_1 - x) \cos \theta + (y_1 - y) \sin \theta = 0$$

$$\frac{x - x_1}{\sqrt{(x - x_1)^2 + (y - y_1)^2}} \cos \theta + \frac{y - y_1}{\sqrt{(x - x_1)^2 + (y - y_1)^2}} \sin \theta = -\frac{r_1}{\sqrt{(x - x_1)^2 + (y - y_1)^2}}$$

Let

$$\text{Atan } 2(x, y) = \begin{cases} \text{sign}(y) \cdot \text{atan} \frac{|y|}{|x|} & x \geq 0 \\ \text{sign}(y) \cdot (\pi - \text{atan} \frac{|y|}{|x|}) & x < 0 \end{cases}$$

be the four quadrant arctangent of elements of x and y , then

$$\cos(\theta_1 - \varphi) = \frac{r_1}{\sqrt{(x - x_1)^2 + (y - y_1)^2}}$$

where $\varphi = \text{Atan } 2(x - x_1, y - y_1)$. So we have

$$\theta_1 = \text{Atan } 2(x - x_1, y - y_1) + \text{Arcos} \frac{r_1}{\sqrt{(x - x_1)^2 + (y - y_1)^2}}$$

$$\theta_2 = \text{Atan } 2(x - x_1, y - y_1) + \pi - \text{Arcos} \frac{r_1}{\sqrt{(x - x_1)^2 + (y - y_1)^2}}$$

and then for the circle center O_1 and radii r_1 , its two tangent points passing through $p(x, y)$ can be expressed as

$$TP(x, y, x_1, y_1, r) = \{(r_1 \cos \theta_1, r_1 \sin \theta_1), (r_1 \cos \theta_2, r_1 \sin \theta_2)\}$$

3.2. Exterior Common Tangents of Two Circles

As shown in Figure 7, O is the intersection point of the two inner common tangents of the two circles with centers O_1, O_2 and radii r_1, r_2 . For the purpose of finding the exterior common tangents of two circles, it is sufficient to find the intersection points of each exterior common tangent and two circles.

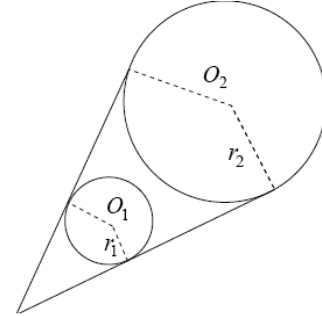


Figure 7: Exterior common tangents of two circles.

The coordinates of intersection point can be expressed as

$$(x, y) = (x_1, y_1) + \lambda(x_1 - x_2, y_1 - y_2)$$

where λ is a constant need to be determined.

If $r_1 < r_2$, we have

$$\frac{|OO_1|}{r_1} = \frac{|OO_1| + |O_1O_2|}{r_2}$$

$$|OO_1| = \frac{r_1 |O_1O_2|}{r_2 - r_1}$$

So we have

$$\lambda = r_1 / (r_2 - r_1)$$

and

$$(x, y) = (x_1, y_1) + \frac{r_1}{r_2 - r_1} (x_1 - x_2, y_1 - y_2) \tag{1}$$

If $r_1 > r_2$, the coordinates of intersection point can be expressed as

$$(x, y) = (x_2, y_2) + \frac{r_2}{r_1 - r_2} (x_2 - x_1, y_2 - y_1)$$

$$= (x_1, y_1) + \frac{r_1}{r_2 - r_1} (x_1 - x_2, y_1 - y_2)$$

Combining the last equation with equation (1), we conclude that the intersection point coordinates of the two inner common tangents of the two circles can

always be expressed equation (1), whether r_1 is bigger than r_2 or not.

After finding the intersection point of the two exterior common tangents, we can find the intersection points of each exterior common tangent and two circles using the method in sub-section 3.1.

3.3. Inner common tangents of two circles

As shown in Figure 7, $O(x, y)$ is the intersection point of the two inner common tangents of the two circles,

$$(x_{11}, y_{11}), (x_{12}, y_{12}) \in TP(x, y, x_1, y_1, r_1)$$

and

$$(x_{21}, y_{21}), (x_{22}, y_{22}) \in TP(x, y, x_2, y_2, r_2)$$

denote two tangent points of inner common tangents is circles O_1 and O_2 respectively, then

$$(x, y) = (x_1, y_1) + \lambda(x_2 - x_1, y_2 - y_1)$$

where λ is a constant need to be determined. Now consider

$$\frac{|OO_1|}{r_1} = \frac{|O_1O_2| - |OO_2|}{r_2}$$

$$|OO_1| = \frac{r_1|O_1O_2|}{r_1 + r_2}$$

We have $\lambda = r_1 / (r_1 + r_2)$, and

$$(x, y) = (x_1, y_1) + \frac{r_1}{r_1 + r_2}(x_2 - x_1, y_2 - y_1)$$

After finding the intersection point of the two inner common tangents, we can find the four intersection points of two inner common tangents and two circles using the method in sub-section 3.1, that is $(x_{11}, y_{11}), (x_{12}, y_{12}), (x_{21}, y_{21})$ and (x_{22}, y_{22}) .

We can conclude that (x_{11}, y_{11}) and (x_{21}, y_{21}) are two points on same inner common tangent if vectors $(x_1, y_1) - (x_{11}, y_{11})$ is parallel to vector $(x_1, y_1) - (x_{21}, y_{21})$.

Using the above algorithms we can find all common tangents of any two circles.

4. SHORTEST COLLISION-FREE PATH ALGORITHM

For the problem of shortest collision-free path planning presented in section 1, we will give an algorithm to find the shortest collision-free path automatically in this section. In order to make it convenient to depict the algorithm, we first give the following definition.

4.1. Definition

A common tangent segment of two circles is called a *collision-free common tangent segment*, if it does not intersect any other circle.

By regarding the point as a circle with radii zero, the definition is the same with tangent of a circle and a point. Therefore, a relative shortest collision-free path is acyclic curve, whose any two adjacent collision-free common tangent segments are consistent with respect the arc between them. If the endpoints of collision-free common tangent segments once are provided orderly, a relative shortest collision-free path will be determined, and so a relative shortest collision-free path can be represented by a sequence of points. For example, the relative shortest collision-free path passing through p_s , circles O_1, \dots, O_k and p_e orderly can be represented as,

$$L = \{p_s, t_1, t_2, \dots, t_{2k-1}, t_{2k}, p_e\}$$

where points t_{2i-1} and t_{2i} are intersection points of the circle O_i and two collision-free common tangent segments $t_{2i-2}t_{2i-1}$ and $t_{2i}t_{2i+1}$ ($i = 1, 2, \dots, k$), they are connected by an arc segment with center O_i and radii r_i .

4.2. Definition

In a relative shortest collision-free path L , the sub-path from a collision-free common tangent segment to end point p_e is called a *remainder path*, and the number of straight line segments contained in path L is called *the index of the path L*.

Actually, for any relative shortest collision-free path and $i = 1, 2, \dots, k$, if we regard the point t_{2i-1} as a node, and the length of path $t_{2i-1}t_{2i}t_{2i+1}$ as the weight of the path, Dijkstra shortest path algorithm [19, 20] and its improved algorithm [21] can be used to find the shortest collision-free path. Let l denote a variable upper bound of the shortest collision-free path length with a large enough initial value. We first connect points p_s and p_e , and obtain a directed straight line segment $p_s p_e$. If the straight line segment $p_s p_e$ does

not intersect the n circles, we take the value of l equal to the length of the straight line segment $p_s p_e$. Then we have found the shortest collision-free path from p_s to p_e with length l . Otherwise, we need to find all the remainder paths with index 1 and length less than l .

For each of the n circles, we can find its collision-free common tangents passing through the end point p_e using the approach produced in sub-section 3.1. Denote the remainder paths with index 1 and length less than l by

$$\{t_{1k}, p_e | k = 1, 2, \dots, i_1\} \quad (1)$$

where t_{1k} lies on the circle with center O_{1k} and radii r_{1k} , and straight line segment $t_{1k} p_e$, namely a remainder path with index 1, is a collision-free common tangent segment of circle O_{1k} and end point p_e , i_1 represents the number of the remainder paths with index 1 and length less than l .

For $k = 1, \dots, i_1$, if there is a collision-free common tangent segments $p_s t_{1k}'$ of circle O_{1k} and starting point p_s , where t_{1k}' lies on the circle O_{1k} , $p_s t_{1k}'$ and $t_{1k} p_e$ are consistent, and the arc $t_{1k}' t_{1k}$ is a inferior arc, then path $\{p_s, t_{1k}', t_{1k}, p_e\}$ is a relative shortest collision-free path. Furthermore, if its length is smaller than l , we take the value of l equal to the length of the path. Apparently, if the value of l once is changed, it will represent the length of the shortest collision-free path has been found.

By property 2.4, a relative shortest collision-free path intersects each of the circles at most once, so the starting points of the remainder path with index 2 and sub-path $t_{1k} p_e$ lie on circle with centers in set $\{O_i | i = 1, 2, \dots, n\} - \{O_{1k}\}$. Since the remainder path with length bigger than l is impossible to be a sub-path of the shortest collision-free path, we denote the set of the remainder paths with index 2 and length less than l by

$$\left\{ t_{2i}, t_{1i}', t_{1k}, p_e \mid k = 1, 2, \dots, i_1, i = \sum_{r=1}^{k-1} j_r + 1, \dots, \sum_{r=1}^k j_r \right\} \quad (2)$$

where point t_{2i} lies on the circle with center

$$O_{2i} \in \{O_i | i = 1, 2, \dots, n\} - \{O_{1k}\}$$

and radii r_{2i} , point t_{1i}' lies on the same circle as the point t_{1k} , straight line segment $t_{2i} t_{1i}'$ is an collision-free common tangent segment of circles O_{1k} and O_{2i} ,

tangent segments $t_{2i} t_{1i}'$ and $t_{1k} p_e$ are consistent, and the arc $t_{1i}' t_{1k}$ is an inferior arc. The starting points of these remainder paths lie on the circles with centers in

$$\{O_{2i} | i = 1, 2, \dots, i_2\}$$

where $i_2 = \sum_{r=1}^{i_1} j_r$. Since for $i = 1, \dots, i_2$, there is only a sub-path from straight line segment $t_{2i} t_{1i}'$ to end point p_e , i_2 represents the number of remainder paths with index 2 and length less than l .

For $i = 1, \dots, i_2$, considering the collision-free common tangent segments $p_s t_{s2}'$ of circle O_{2i} and starting point p_s , where t_{s2}' lies on the circle O_{2i} . If $p_s t_{s2}'$ and $t_{2i} t_{1i}'$ are consistent, and the arc $t_{s2}' t_{2i}$ is an inferior arc, then path $\{p_s, t_{s2}', t_{2i}, t_{1i}', t_{1k}, p_e\}$ is a relative shortest collision-free path. If its length is smaller than l , we take the value of l equal to length of the path.

By property 2.4, the starting points of the remainder path with index 3 lie on circle with centers in set $\{O_i | i = 1, \dots, n\} - \{O_{1k}, O_{2i}\}$. For

$$O_{31} \in \{O_i | i = 1, \dots, n\} - \{O_{1k}, O_{2i}\}$$

let $t_{31} t_{21}'$ be a collision-free common tangent segment of circles O_{31} and O_{2i} , where t_{31} and t_{21}' lie on the circles O_{31} and O_{2i} respectively. If the tangent segment $t_{31} t_{21}'$ may be connected to many sub-paths given in expression (2) to form the remainder paths with index 3, we delete other sub-paths except the shortest one, such that starting from the tangent segment $t_{31} t_{21}'$, there is only a remainder path with index 3. Denote the remainder paths with index 3 and length less than l by

$$\{t_{3j}, t_{2j}', t_{j(2)}, t_{j(1)}', t_{j(1)}, p_e | j = 1, 2, \dots, i_3\} \quad (3)$$

where i_3 represents the number of remainder paths with index 3 and length less than l .

We need to repeat this process until we obtain a positive integer N , such that $i_1 > 0, \dots, i_{N-1} > 0, i_N = 0$.

Since equation $i_N = 0$ means that except the path found with length l , the remainder path with index N does not exist or its length is bigger than l . Then the path with length l is the shortest collision-free path.

5. ALGORITHM DESCRIPTION IN A STYLE OF PSEUDO-CODE

Denote the shortest one of the index v remainder paths starting from the straight line segment $t_{vi}t_{(v-1)i}'$ to end point p_e by $s_i^{(v)}$. Using the algorithms given in Section 3, we can obtain $s_i^{(v+1)}$ ($i=1, \dots, i_{v+1}$) from $s_i^{(v)}$ ($i=1, \dots, i_v$), as shown in Section 4. The process can be expressed as the following operator:

$$(s_1^{(v+1)}, \dots, s_{i_{v+1}}^{(v+1)}) = \text{ExtendPath}(s_1^{(v)}, \dots, s_{i_v}^{(v)})$$

For example in Section 4,

$$(s_1^{(1)}, \dots, s_{i_1}^{(1)}) = \{t_k, p_e | k=1, 2, \dots, i_1\}$$

$$\left\{ t_{2i}, t_{1i}', t_{1k}, p_e \mid k=1, 2, \dots, i_1, i = \sum_{r=1}^{k-1} j_r + 1, \dots, \sum_{r=1}^k j_r \right\}$$

$$= \text{ExtendPath} \{t_k, p_e | k=1, 2, \dots, i_1\}$$

Using the above operator, the pseudo-code for the shortest collision-free path algorithm is as follows.

Input. n circles with centers O_1, \dots, O_n and radii r_1, \dots, r_n respectively, the starting point p_s and the end point p_e of the manipulator's effectors.

Output. The shortest collision-free path s from starting point p_s to end point p_e .

1. Initialize l as a constant bigger than the length of some a path from p_s to p_e .
2. If the straight line segment $p_s p_e$ does not intersect the n circles, let l be equal to the length of the straight line segment $p_s p_e$. Then let $s = \{p_s, p_e\}$, go to step 7.
3. Find all the remainder paths with index 1 and length less than l , denote them by

$$s_i^{(1)} \quad (i=1, \dots, i_1).$$

Let $v=1, t_{0i}' = p_e \quad (i=1, \dots, i_1)$.

4. If $i_v = 0$, go to step 10.
5. For $i=1, \dots, i_v$, if $p_s t_{vi}''$ and $t_{vi} t_{(v-1)i}'$ are consistent, and the arc $t_{vi}'' t_{vi}$ is an inferior arc, Then let

$$s = \{p_s, t_{vi}'' , s_i^{(v)}\},$$

and let l be equal to the length of path s .

6. Compute

$$(s_1^{(v+1)}, \dots, s_{i_{v+1}}^{(v+1)}) = \text{ExtendPath}(s_1^{(v)}, \dots, s_{i_v}^{(v)}).$$

Set $v \leftarrow v+1$, go to step 4.

7. Input s .

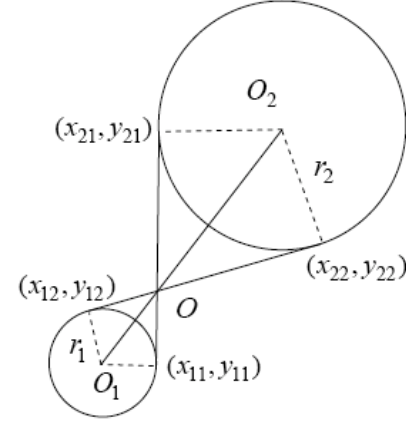


Figure 8: Inner common tangents of two circles.

6. SIMULATION

The shortest collision-free path problem is shown in Figure 7. In Figure 7, different line types represent the starting tangent segment of a remainder path with different index. Some of these tangent points have been lined out in Figure 7. According to index order, the centers of the circles on which the starting points of remainder paths lie are given as follows

$$O_{11} = O_{12} = O_5$$

$$O_{13} = O_{14} = O_6$$

$$\{O_{2k} | k=1, 2, \dots, i_2\} = \{O_2, O_3, O_4\}$$

$$\{O_{3k} | k=1, 2, \dots, i_3\} = \{O_2, O_3, O_4\}$$

$$\{O_{4k} | k=1, 2, \dots, i_4\} = \{O_1\}$$

After all starting points of remainder paths index 2 are obtained, we take the value of l equal to the length of path $\{p_s, t_{s2}', t_{26}, t_{16}', t_{14}, p_e\}$. After all starting points of remainder paths index 4 are obtained, we take the value of l equal to the length of path

$$\{p_s, t_{41}', t_{41}, t_{31}', t_{31}, t_{21}', t_{24}, t_{14}', t_{13}, p_e\}$$

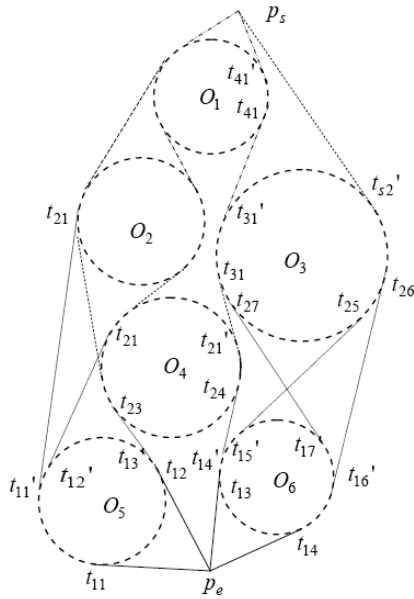


Figure 9: An algorithm sketch map of shortest collision-free path.

After this, the lengths of all remainder paths with index 5 are bigger than l , which means $i_5 = 0$. So the shortest collision-free path is

$$\{p_s, t_{41}', t_{41}, t_{31}', t_{31}, t_{21}', t_{24}, t_{14}', t_{13}, p_e\}$$

7. THE GENERALIZATION TO THE SLENDER OBSTACLE REGION

In the previous sections, we assume that the obstacle regions are n disjoint circles. But not all of the obstacle regions are circular in general. Expanding each of the non-circular obstacle regions into a circle and replacing the original obstacle regions by the circles, we can still obtain n circles. As long as the n circles are disjoint, a shortest collision-free path based on the n disjoint circles can be found using the method given in previous sections. However, if the original obstacle region is slender, its expanded circle will be possible to intersect the other circles as shown in Figure 10, where two obstacle regions are expanded into two intersectant circles O_1 and O_2 . In order to ensure that all the circles will not intersect, we will expand the obstacle region A in Figure 10 into the region surrounded by two circles O_3 , O_3 and their two exterior common tangent segments L_1 and L_2 . The circles O_1 , O_3 and O_3 will be called *expanded circles*.

However, it should be pointed out that the “slender” obstacle region is a relative concept relevant to the distribution of its neighbouring obstacle regions. After an obstacle region is expanded into a circle, if the circle does not intersect any expanded circle, it is not necessary to consider it as a slender obstacle region.

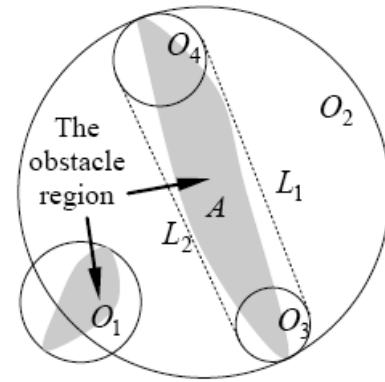


Figure 10: The intersection of two expanded circular obstacle region.

In the path planning process, the obstacle region A can be replaced by the two circles O_3 and O_4 , but then, an additional restriction needs to be appended to the common tangent segments in path, that is, except for the complete coincidence cases they do not intersect the two tangent segments L_1 and L_2 . In fact, if each common tangent segments in path do not intersect L_1 and L_2 , the path will not traverse the obstacle region A in Figure 10.

For each slender obstacle region we can find two circles and their two common tangent segments, such that the slender obstacle region is surrounded by the two circles and their two exterior common tangent segments. For the other obstacle regions we can expand them into some circles with different centers and radii. In this way, we can obtain some circles and exterior common tangent segments called *obstacle common tangent segments*.

Let A_1, A_2, \dots, A_m be m obstacle regions, where A_1, A_2, \dots, A_{m_1} are $m_1 (< m)$ slender obstacle regions. Suppose that obstacle region $A_i (i = 1, 2, \dots, m_1)$ is expanded into the region surrounded by the two circles O_{2i-1}, O_{2i} and their two exterior common tangent segments L_{2i-1}, L_{2i} , and that obstacle region $A_i (i = m_1, m_1 + 1, \dots, m)$ is expanded into the circular region O_{2m_1+i} . In this way, we can obtain n expanded circles and N obstacle common tangent segments, where $n = m + m_1$, $N = 2m_1$.

Under the restriction that each common tangent segment in path does not intersect the N obstacle common tangent segments, we can find a shortest collision-free path based on the n expanded circles by the method developed in the previous sections. The path is also a feasible collision-free path for the m obstacle regions A_1, A_2, \dots, A_m , despite the fact it is not

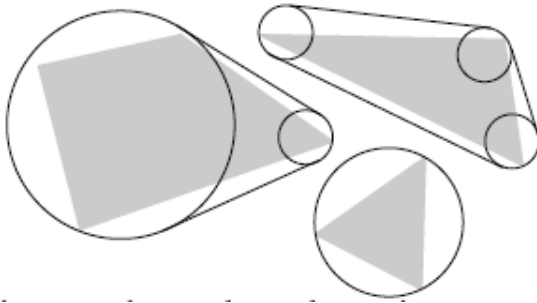


Figure 11: Three obstacle regions surrounded by various numbers of circles and common tangent segments.

the shortest path. However, for any obstacle region, we can choose more circles and common tangent segments to surround it, as shown in Figure 11, and that with the increase of the numbers of the circles and the common tangent segment and the reduction of the radii of the circles, the region surrounded by the circles and the common tangent segments can be made to approach the obstacle region more closely. Thus it can be seen that under the restriction that each common tangent segment in path does not intersect these obstacle common tangent segments, the shortest collision-free path based on these expanded circles, obtained using the method developed in the previous sections, will approach the shortest collision-free path based on the obstacle regions.

8. CONCLUSIONS

This paper presents a method for planning collision-free paths based on circular obstacle region. A series of simulations demonstrated that the proposed methods might effectively establish shortest collision-free paths in two dimensions for an acceptable short time for the generation of paths. Despite the fact that an obstacle region can be surrounded by a circle with big-enough radii, a circle cannot surround an obstacle region as closely as an ellipse, especially in the case of the slender obstacle region. However, it is a very difficult to find the shortest collision-free paths based on ellipse obstacle regions, which includes computing arc length of an ellipse and the common tangent of two ellipses. These issues will be addressed in future.

ACKNOWLEDGEMENT

This work was supported by National Basic Research Program of China (No. 2013CB733000)

REFERENCES

- [1] Evangelos P, Iakovos P and Ioannis P. Polynomial-based obstacle avoidance techniques for nonholonomic mobile manipulator systems J. Robotics and autonomous systems 2005; 51: 229-247. <http://dx.doi.org/10.1016/j.robot.2005.03.006>
- [2] Ogren P, Leonard NE. A convergent dynamic window approach to obstacle avoidance [J]. IEEE Trans on robotics and automation 2005; 21(2): 188-195. <http://dx.doi.org/10.1109/RO.2004.838008>
- [3] Falen BR, Warren WH. Behavioral dynamics of steering, obstacle avoidance, and route selection [J]. Journal of experimental psychology: Human perception and performance 2003; 29(2): 343-362. <http://dx.doi.org/10.1037/0096-1523.29.2.343>
- [4] Fajen BR, Warren WH, Termizer S, et al. A dynamical model of steering, obstacle avoidance, and route selection [J]. International Journal of Computer Vision 2003; 54(1/2): 13-34. <http://dx.doi.org/10.1023/A:1023701300169>
- [5] Hart PE, Nilsson NJ, Raphael B. A formal basis for the heuristic determination of minimum cost paths [J]. IEEE Trans Syst Sci Cybern 1968; 4: 100-107. <http://dx.doi.org/10.1109/TSSC.1968.300136>
- [6] Tatsuya O, Pipaporn E, Liang Z, Hiroshi N. An A* Algorithm Framework for the Point-to-Point Time-Dependent Shortest Path Problem [J]. Lecture notes in computer science 2011; 7033(1): 164-175.
- [7] Takahashi O, Schilling RJ. Motion planning in a plane using generalized Voronoi diagrams [J]. IEEE Trans Robot Autom 1989; 11: 143-150. <http://dx.doi.org/10.1109/70.88035>
- [8] Hou E, Zheng D. Mobile robot path planning based on hierarching hexagonal decomposition and artificial potential fields [J]. Robot Syst 1994; 11: 605-614. <http://dx.doi.org/10.1002/rob.4620110704>
- [9] Schwartz JT, Sharir M. On the Piano Movers' problem: I. The case if a two-dimensional rigid polygonal body moving amidst polygonal barriers [J]. IEEE Trans Robot Autom 1983; 36: 345-398. <http://dx.doi.org/10.1002/cpa.3160360305>
- [10] Valavanis KP, Hebert T, Kolluru R, Tsourveloudis N. Mobile robot navigation in 2-D dynamic environments using an electrostatic potential field [J]. IEEE Trans. Syst., Man, Cybern. A 30 (2000); 187-196.
- [11] Russell S, Norvig P. Artificial intelligence: a modern approach [M]. USA, New Jersey: Prentice Hall (1995).
- [12] Dorigo M, Bonabeau E, Theraulaz G.. Ant algorithms and stigmergy[J]. Future generation computer systems 2000; 16: 851-871. [http://dx.doi.org/10.1016/S0167-739X\(00\)00042-X](http://dx.doi.org/10.1016/S0167-739X(00)00042-X)
- [13] Gemeinder M, Gerke M. GA-based path planning for mobile robot systems employing an active search algorithm. Applied soft computing 2003; 3: 149-158. [http://dx.doi.org/10.1016/S1568-4946\(03\)00010-3](http://dx.doi.org/10.1016/S1568-4946(03)00010-3)
- [14] Tian L, Collins C. An effective robot trajectory planning method using a genetic algorithm [J]. Mechatronics 2004; 14: 455-470. <http://dx.doi.org/10.1016/j.mechatronics.2003.10.001>
- [15] Huseyin C, Halim C. A hybrid harmony search and TRANSYT hill climbing algorithm for signalized stochastic equilibrium transportation networks J. Transportation research part C: emerging technologies 2012; 25(12): 152-167.
- [16] Jonathan A and Manuel V. Steepest ascent hill climbing for portfolio selection J. Lecture notes in computer science 2012; 7248(1): 145-154.
- [17] Krispin A, Davies A and Graeme N. Rapid control selection through hill-climbing methods J. Lecture notes in computer science 2012; 7507(1): 571-580.
- [18] Mark de B, Otfried C, Marc van K, Mark O. Computational geometry: algorithms and applications M. Berlin Heidelberg: Springer-Verlag, 2008.

- [19] Neaimeh M, Hill G, Hübner Y, et al. Routing systems to extend the driving range of electric vehicles J. IET Intelligent Transport Systems 2013; 7(3): 327-336.
<http://dx.doi.org/10.1049/iet-its.2013.0122>
- [20] Klie T, Straub F. Integrating SNMP Agents with XML-based Management Systems J. IEEE Communications Magazine, 2004; 42(7): 76-83.
<http://dx.doi.org/10.1109/MCOM.2004.1316537>
- [21] An K, Zheng YL and, Qiu ZL. A New Algorithm Solution to the Shortest Path Problem of Weighting Directed Graph-Method of Forward Graph J. Journal of Hebei Normal University(Natural Science Edition) 2000; 24(1): 23-24.(in Chinese).

Received on 05-06-2015

Accepted on 07-07-2015

Published on 31-07-2015

DOI: <http://dx.doi.org/10.15377/2409-9694.2015.02.01.3>

© 2015 An Kai; Avanti Publishers.

This is an open access article licensed under the terms of the Creative Commons Attribution Non-Commercial License (<http://creativecommons.org/licenses/by-nc/3.0/>) which permits unrestricted, non-commercial use, distribution and reproduction in any medium, provided the work is properly cited.